PERSPECTIVES: NANOTUBES

Burn and Interrogate

Mildred S. Dresselhaus

Carbon nanotubes have a special place in nanoscale science. They are simple enough for detailed calculations and predictions and promising for nanotechnology because of their unique properties, such as small diameter (1 to 2 nm), long length (many micrometers), high mechanical strength, high thermal and chemical stability, and excellent heat conduction. Furthermore, nanotubes can be either metallic or semiconducting, with semiconducting band gaps that can be controlled through the tube diameter. The reports by Ouyang *et al.* on page 702 (*1*) and Collins *et al.* on page 706 (*2*) in this issue of *Science* advance our knowledge of the nanotube conduction process substantially and help us move toward applying this knowledge in nanoelectronics.

Even before single-wall carbon nanotubes (SWNTs) had been synthesized for the first time, calculations based on the symmetry of the honeycomb lattice of graphite predicted that they could be either semiconducting or metallic depending on their geometry. Nanotubes are typically described by two integers (n,m) that specify the tube diameter

$$d_t = \sqrt{3}\, a_{C\text{–}C}\,(n^2 + mn + m^2)^{1/2}/\pi \qquad (1)$$

where $a_{C\text{–}C}$ is the carbon-carbon bond length, and the chiral angle

$$\theta = \tan^{-1}[\sqrt{3}m/(m + 2n)] \qquad (2)$$

which gives the orientation of the carbon hexagons with respect to the tube axis (*3*). Early on, the prediction that nanotubes could be metallic ($n - m = 3q$, where q is an integer) led to discussions of their stability. In particular, the question was raised whether curvature-related effects would lead to the formation of a minigap at the Fermi level (*4*, *5*) depending on nanotube chirality and diameter. Only (n,n) armchair nanotubes with a chiral angle $\theta = 30°$ were expected to have a stable metallic state, whereas zigzag ($\theta = 0°$) and chiral nanotubes ($0° < \theta < 30°$) were expected to develop small band gaps as a result of curvature-related effects (*4*).

Ouyang *et al.* (*1*) report the first experimental observations of minigaps arising from curvature-related effects, using low-temperature (about 5 K) scanning tunneling spectroscopy (STS). Prior STS experiments (*6*, *7*) confirmed that nanotubes could be either metallic (with no band gap) or semiconducting (with a band gap of hundreds of millivolts), verified the presence of sharp singularities in the one-dimensional density of states of carbon nanotubes, and showed a much larger energy separation E_{11} between the lowest conduction band singularity and highest valence band singularity for metallic nanotubes compared with semiconducting nanotubes, characteristics that are used to distinguish metallic from semiconducting tubes (see the figure). It has also been shown experimentally (*6*) and theoretically (*8*) that these singularities exhibit a dependence on the chiral angle, which yields a unique set of interband energy separations for each (n,m) SWNT. This has led to the development of a noninvasive resonance Raman scattering method to determine the (n,m) indices (*9*) of individual, isolated SWNTs.

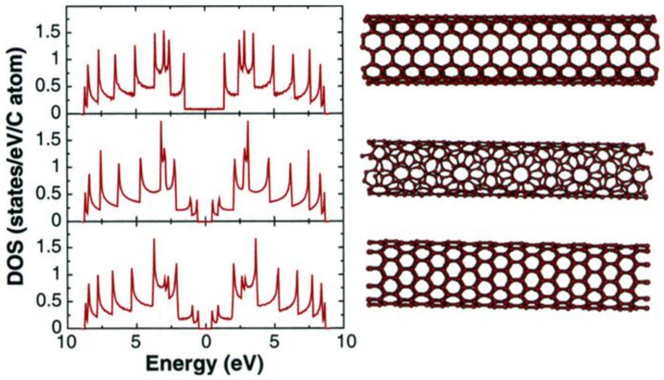

How to distinguish different nanotubes. The density of electronic states for a metallic (6,6) armchair nanotube (**top**), a semiconducting (8,3) chiral nanotube (**middle**), and a semiconducting (11,0) zigzag nanotube (**bottom**), showing sharp singularities. Calculated without including the effect of nanotube curvature (*3*). The effect of nanotube curvature is to open a minigap at the Fermi level, *E* = 0.

CREDIT: RIICHIRO SAITO/ELECTROCOMMUNICATIONS UNIVERSITY, TOKYO

Ouyang *et al.* (*1*) measure the local electronic density of states of nanotubes with (n,m) values determined by scanning tunneling microscopy (STM). They show that in the case of zigzag $(n,0)$ nanotubes, a minigap proportional to $1/d_t^2$ forms at the Fermi level because of curvature-related effects, consistent with theory (*1*, *4*, *10*). Also as expected, isolated armchair (n,n) nanotubes have no curvature-induced minigap (*1*, *3*, *11*). But intertube interactions within an SWNT bundle result in the opening of a "pseudogap" that is proportional to $1/d_t$, and this pseudogap is even larger magnitude than the minigap of an isolated zigzag tube of the same d_t.

These experimental results will stimulate further theoretical and experimental research, including more detailed calculations of the dependence of minigaps on nanotube diameter and chiral angle. This should lead to a better understanding of the role of chirality in determining the physical properties of SWNTs. For example, simple theoretical models predict a constant electronic density of states (DOS) over the energy range of E_{11} for armchair nanotubes (see the figure) (*3*), but it remains to be shown whether experiment and more detailed theory support this prediction for metallic tubes and, if so, how this constant DOS depends on diameter and chirality outside the minigap region but within the E_{11} range. Another example is provided by nanotubes with very small diameters. At $d_t < 0.7$ nm, simple predictions about semiconducting and metallic behavior are expected to break down (*11*); for example, the (5,0) tube, for which $n - m$ is not divisible by 3, is now expected to be semimetallic. The synthesis of very small-diameter nanotubes with (n,m) values of (5,0) and (3,3) has been reported with the use of zeolite templates (*12*). The ability to measure minigaps experimentally will likely lead to a systematic experimental and theoretical examination of the DOS for these small-diameter nanotubes. Because the experimental minigaps reported by Ouyang *et al.* (*1*) are large compared with k_BT (k_B, Boltzmann constant; T, temperature) at room temperature, they might be important for device applications of metallic nanotubes.

The realization of a practical nanotube-based electronic device is brought substantially closer to reality by Collins *et al.* (*2*). To use an SWNT rope for field-effect transistor (FET) applications, the metallic tubes must be removed, lest they prevent switching action by the gate field. Yet Collins *et al.*'s technique allows the fabrication of carbon nanotube FETs from ropes of SWNTs containing both metallic and semiconducting nanotubes without having to separate the two types of tubes or to prealign or ori-

---

The author is at the Department of Physics and the Department of Electrical Engineering and Computer Science, Massachusetts Institute of Technology, Cambridge, MA 02139, USA. E-mail: millie@mgm.mit.edu

ent them. The underlying idea is simple. Metallic carbon nanotubes can withstand very high current densities (10^9A/cm^2), but at high enough currents the nanotubes will burn up in air. In this way, metallic tubes can be removed selectively from SWNT ropes. Individual nanotube shells can also be removed, one at a time, from multiwalled nanotubes (MWNTs) (*2*). The use of shell-by-shell breakdown of an MWNT to determine the electrical properties of its individual shells is also demonstrated (*2*). By taking advantage of the $1/d_t$ dependence of the band gap of semiconducting shells, FETs with desired band gaps can be produced.

Collins *et al.* (*2*) first use a gate electrode to effectively deplete the electrical carriers (electrons or holes) from the semiconducting tubes within a SWNT rope. The metallic SWNTs within the rope can then be destroyed by current-induced oxidation, leaving the carrier-depleted semiconducting tubes, which carry no current, intact. To fabricate dense arrays of FETs, the SWNT ropes are deposited on an oxidized Si wafer, which also serves as the back gate. An array of source, drain, and side-gate electrodes is then fabricated lithographically on top of the permanently modified SWNT ropes. The concentration of the tubes is preadjusted so that on the average, there is one SWNT rope bridging the source and drain. The back gate (the wafer itself) is used to deplete the semiconducting tubes, followed by the application of a stress voltage to destroy the metallic tubes in the ropes. Dense arrays of nanotube FETs are thus produced in a self-assembly process. The minigaps and pseudogaps observed in STM/STS studies (*1*) do not seem to impede the processing steps of the FETs (*2*).

Both the low-temperature STS/STM studies (*1*) and the selective current-induced removal of nanotube shells (*2*) provide new ways to study the dependence of the electronic DOS on nanotube diameter and chiral angle. Presently, there is no experimental method for synthesizing carbon nanotubes with a specified chiral angle, although progress has been made with achieving some degree of selectivity of the nanotube diameter by controlling growth process parameters, such as growth temperature, carrier gas mixture, and catalyst selection. A recent breakthrough (*13*) showing how to prepare self-assembled bundles of metallic (10,10) armchair nanotubes offers promise that selectivity of nanotube diameter and chiral angle is possible.

Better knowledge of the dependence of physical properties on chiral angle may some day lead to the utilization of some highly sensitive property to selectively control the chiral angle and diameter in the nanotube growth process, so that desired metallic or semiconducting tubes can be grown at will.

References and Notes

1. M. Ouyang, J.-L. Huang, C. L. Cheung, C. M. Lieber, *Science* **292**, 702 (2001).
2. P. G. Collins, M. S. Arnold, P. Avouris, *Science* **292**, 706 (2001).
3. R. Saito, G. Dresselhaus, M. S. Dresselhaus, *Physical Properties of Carbon* Nanotubes (Imperial College Press, London, 1998).
4. N. Hamada, S. Sawada, A. Oshiyama, *Phys. Rev. Lett.* **68**, 1579 (1992).
5. R. Saito, M. Fujita, G. Dresselhaus, M. S. Dresselhaus, *Phys. Rev. B* **46**, 1804 (1992).
6. T. W. Odom, J. L. Huang, P. Kim, C. M. Lieber, *Nature* **391**, 62 (1998).
7. J. W. G. Wildöer, L. C. Venema, A. G. Rinzler, R. E. Smalley, C. Dekker, *Nature* **391**, 59 (1998).
8. R. Saito, G. Dresselhaus, M. S. Dresselhaus, *Phys. Rev. B* **61**, 2981 (2000).
9. A. Jorio *et al.*, *Phys. Rev. Lett.* **86**, 1118 (2001).
10. J. X. Cao, X. H. Yan, J. W. Ding, D. L. Wang, *J. Phys. Condens. Matter* **13**, L271 (2001).
11. S. G. Louie, in *Carbon Nanotubes: Synthesis, Structure, Properties and Applications*, M. S. Dresselhaus, G. Dresselhaus, P. Avouris, Eds. (Springer, Berlin, 2001), pp. 113–146.
12. T. W. Tombler *et al.*, *Nature* **405**, 769 (2000).
13. R. R. Schlittler *et al.*, *Science* 5 April 2001 (101126/science.1057823).

14. I gratefully acknowledge helpful discussions with G. Dresselhaus, R. Saito, and other colleagues and support from NSF grant DMR 98-04734.

PERSPECTIVES: BIOINORGANIC CHEMISTRY

Oxygenase Pathways: Oxo, Peroxo, and Superoxo

Lawrence Que Jr. and Yoshihito Watanabe

Many key metabolic transformations require the controlled oxidation of organic species. These transformations often rely on the activation of molecular oxygen, O_2, by metal ions in the active sites of oxygenase enzymes. At a recent symposium on "Oxygen Activation by Metalloenzymes and Their Models" (*1*), highlighted in this perspective, two themes threaded through a number of the talks: a common oxygen activation scheme and the importance of O_2 in posttranslational modification of proteins.

Oxygen activation can occur at mononuclear heme (porphyrin) sites, nonheme monoiron and diiron sites, mononuclear and dinuclear copper sites, and even at a heterodinuclear heme-copper site. Despite this diversity of active sites, a common mechanistic hypothesis for oxygen activation is emerging. In this unified scheme, oxygen first binds to a reduced metal center; a metal-peroxo intermediate is then formed, followed by O-O bond cleavage to form a high-valent metal-oxo oxidant that carries out substrate oxidation (see the first figure). The extent to which the catalytic cycle of an enzyme (and its corresponding model compounds) follows this mechanism varies from enzyme to enzyme.

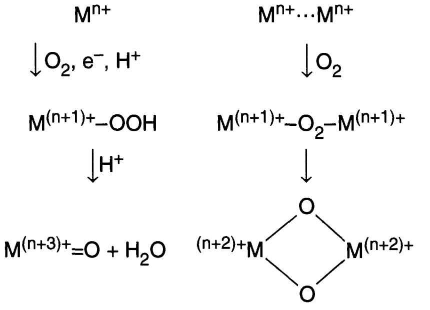

Toward a unified mechanism. Scheme for oxygen activation at metalloenzyme active sites.

The heme enzyme cytochrome P450 is one of the most widely studied systems in bioinorganic chemistry. A high-valent iron-oxo species has generally been thought to be the oxidant responsible for P450-catalyzed oxygenation, but the possibility that an iron-peroxo species may also be involved in some reactions has been raised. For example, Wonwoo Nam (Ehwa Womens University, Seoul, Korea) presented evidence that synthetic iron complexes of highly halogenated, electron-deficient porphyrins catalyze oxygenation reactions through either iron-peroxo or iron-oxo species (*2*). To shed further light on this question, Yoshihito Watanabe (Institute for Molecular Science, Okazaki, Japan) used site-directed mutagenesis to redesign the oxygen carrier myoglobin into a P450-like monooxygenase that can catalyze olefin epoxidation (*3*). Kinetic studies showed that the formation of a high-valent iron-oxo intermediate was the rate-determining step, thus excluding the Fe(III)-OOH (peroxo) intermediate as the oxidant under these conditions. Further evidence comes from studies by Brian Hoffman (Northwestern

---

L. Que Jr. is at the Department of Chemistry, University of Minnesota, Minneapolis, MN 55455, USA. E-mail: que@chem.umn.edu Y. Watanabe is at the Institute for Molecular Science, Okazaki 444-8585, Japan. E-mail: yoshi@ims.ac.jp